Sharks, shark cartilages and shark teeth: A collaborative Africa-USA study to attempt to induce "*Bone: formation by autoinduction*" in cartilaginous fishes

SADJ Feb 2018, Vol 73 no 1 p11

U Ripamonti[1], L Roden[2], B van den Heever[3]

Histological examination of selected shark tissues with notes on the extraction and purification of shark cartilaginous protein extracts.

Sharks belong to the superclass *Gnathostomata* (jawed vertebrates), class *Chondrichthyes* (cartilaginous fishes), and subclass *Elasmobranchii* (sharks, skates and rays). Sharks are classified into eight orders of which *Carchariniforms* are well spread throught the oceans. A phylogenetic investigation of twenty-four species of *Carchariniform* sharks showed that most of the existing lineages of *Carchariniformes* originated in the late Eocene to early Oligocene period (28 to 37 MYBP).[42] The oldest fossilized shark remains are placoid scales from the Harding sandstone (late Ordovician ~ 450 MYBP) of Colorado.

Elasmobranchs possess physiological feature that make them unique amongst fishes: a cartilaginous endoskeleton, with no ribs, a cartilaginous jaw which is not connected to the skull (chondrocranium)[20] (Figs.5,6), and a cartilaginous back bone or chondrocranium engineered of cartilage to protect the cerebral ganglia of the animal (Fig. 7D). The shark uses body undulations to propel its mass through water *via* the use of large muscles enveloping the endoskeleton and also possesses an "active skin". The skin, covered by placoid scales (dermal denticles or odontodes) is connected to thrust-producing muscles through myosepta. (Figs. 1A,8).

Figure 5

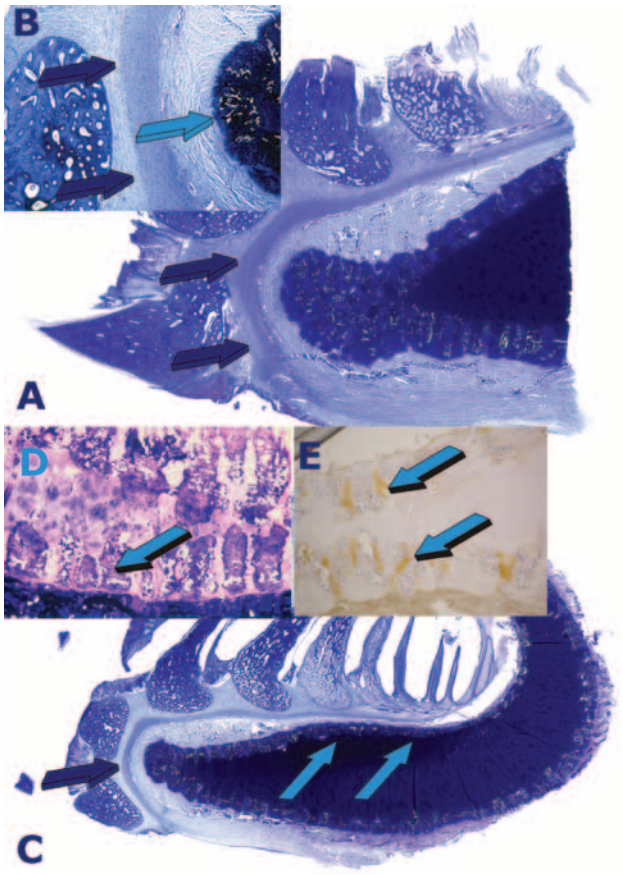

Figure 5. *Shark' jaws, mineralized cartilages, the tesserae, and the conveyor belt moving the teeth forward along the jaw of* Car-

1. Ugo Ripamonti, *MD, PhD Director*, Bone Research Laboratory, Department of Oral Medicine & Periodontology, School of Oral Health Sciences, Faculty of Medicine, University of the Witwatersrand Johannesburg
2. Laura Roden, *BSc (Hons) MSc, PhD.* Bone Research Laboratory, Department of Oral Medicine & Periodontology, School of Oral Health Sciences, Faculty of Medicine, University of the Witwatersrand Johannesburg, present address, Department of Molecular and Cellular Biology, University of Cape Town, Private Bag Rondebosch, 7701 Cape Town, South Africa
3. Barbara van den Heever, *(DMTech) Diploma Medical Technology.* Bone Research Laboratory, Department of Oral Medicine & Periodontology, School of Oral Health Sciences, Faculty of Medicine, University of the Witwatersrand Johannesburg

Corresponding Author
Ugo Ripamonti, Director: Bone Research Laboratory, Faculty of Health Sciences, University of the Witwatersrand, Johannesburg. 2193 Parktown, South Africa +27 11 717 2144 e mail ugo.ripamonti@wits.ac.za

charinus obscurus *specimens. Low power view of* C. obscurus*' jaws with multiple teeth moving forward as set by the conveyor belt above the mineralized tesserae the jaw.* ***A****: A conveyor belt-like structure (****dark blue*** *arrows) sets the teeth forward as described in the text.* ***B****: High power view depicting the conveyor belt (****dark blue*** *arrows) between the roots of the Selachian's teeth (left) and the mineralized cartilage (right,* ***light blue*** *arrow). Mineralized areas are named tesserae as magnified in Inset* ***D*** *(****light blue*** *arrow).* ***C****: Transversal section of* C. obscurus *cartilaginous jaw depicts several forward moving teeth along the conveyor belt (****dark blue*** *arrow).* ***E****: TGF-β_3 immunolocalization (****light blue*** *arrows) within the mineralized tesserae of the Selachian's cartilaginous jaw. Undecalcified sections, toluidine blue stain.*

Figure 6

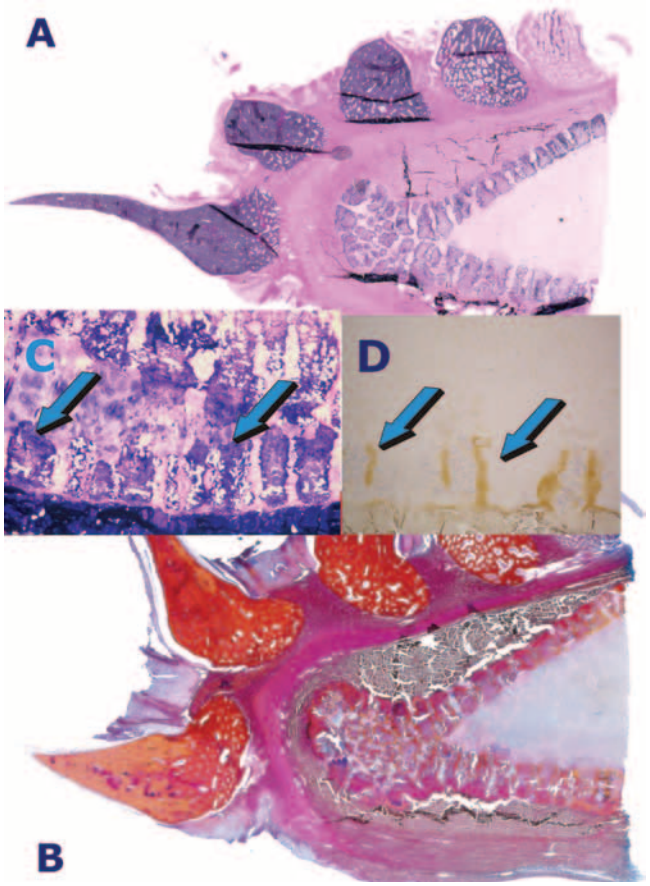

Figure 6*. Low power views of* Carcharinus obscurus *jaws.* ***A****: Mineralized cartilage tesserae (****light blue*** *arrows) and Inset* ***C*** *(****light blue*** *arrows) in close relationship with the conveyor belt (****dark blue*** *arrows in* ***B****) moving forward the continuously erupting teeth along the profile of the mineralized cartilage jaw.* ***D****: Immunolocalization TGF-β_3 (****light blue*** *arrows) within the mineralized tesserae of the cartilaginous jaw. Undecalcified sections, Verhoeffs' stain.*

Figure 7

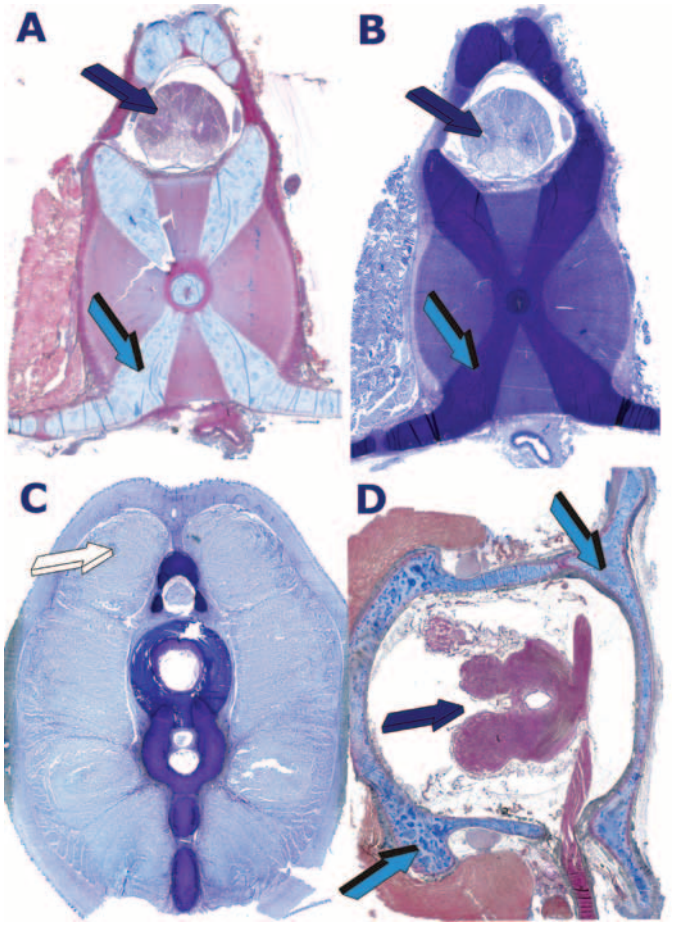

Figure 7. Low power views of the shark vertebral area, enveloping muscle and chondrocrania (**D**). **A,B**: Vertebrae with mineralized areas (***light blue*** arrows) acroos the cartilage body also showing the cartilaginous protected ganglia of the *Selachian*'s body (***dark blue*** arrows). **C**: Transversal section of *C. obscurus* caudal area showing the large muscular mass (***white*** arrow) which propels the rapid undulatory movements of the *Selachian* fish. **D**: Transversal section through the chondrocranium of C. obscurus illustrating the cartilaginous tissues surrounding the ganglia of the *Selachian*'s rudimentary nervous system. Undecalcified sections, **A**,**D** Goldner's trichrome; **B**,**C** toluidine blue.

Figure 8

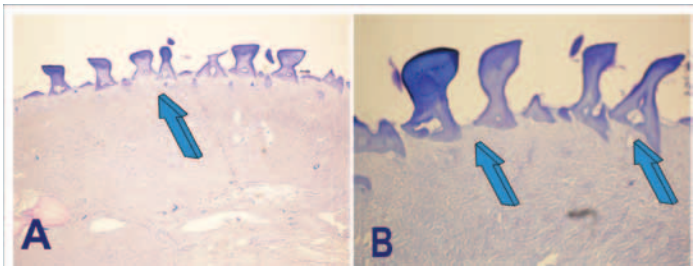

Figure 8.*. Low power views of* Carcharinus obscurus *integument depicting the skin denticles embedded within the subjacent connective tissue stroma of the shark' skin (****light blue*** *arrows).*

The entire endoskeleton of the shark is composed of cartilage which may be mineralized to varying degrees with hydroxyapatite calcium phosphate crystals.[43] The cartilaginous endoskeleton appears to be of functional importance related to the need to main-

tain a stiff yet flexible endoskeleton[44] allowing for rapid undulating forward movements deep in the oceans. Type II collagen, proteoglycans and water are the main components of the elasmobranch cartilages. Types I and II collagens are responsible for the strength and stiffness of the endoskeleton.[45] Notably, proteoglycans do have an inhibitory effect on the calcification of cartilage.[46] Degradation of the proteoglycans by lysosomal enzymes results in calcification.[47] Shark cartilage is strengthened in the jaws and vertebrae by small calcified areas called "*tesserae*" (Figs. 5D,6A). Tesserae in sharks may occur in the jaws, gill arches, chondrocrania (a cartilaginous box containing the neural ganglia of the animal), vertebral centra (Figs. 7A,B), and the supporting cartilages of the fins and claspers.[48] Tesserae are mainly localized at the periphery of the cartilaginous jaws (Figs. 5D,6A). Note that TGF-β_3 immunolocalizes within the tesserae of the cartilaginous jaws (Figs. 5D, 6A). There are three types of cartilaginous mineralization: areolar calcification, a compactly calcified tissue which is found in the vertebral centra (Figs. 7A, B), and prismatic and globular calcifications which may both occur in the blocks of mineralized tissue of the tesserae.[49]

Sharks are polyphyodont, replacing teeth continuously throughout life. Their teeth are not fused to the jaws and are shed at regular intervals with rows or sets of teeth being replaced from behind in a "conveyor belt"-like progression by newly formed teeth as the shark grows or the anterior teeth become worn, broken or lost in predatory acts. (Figs. 4-6).

Still unresolved are the molecular forces which create the forward movement of the teeth. This conveyor belt mechanism was first described by Grady.[4] Tractional forces are possibly initiated by interactions between cell and cell and between cells and extracellular matrix, propelling forward the conveyor belt and with it, all the dentition which has erupted along the belt-like tissue. High power histological examination of undecalcified whole mount sections display the mechanism just below the embedded roots of the *Selachians*' teeth and above the margin of cartilage matrix, with calcified tesserae along the jaws (Figs. 5A-D). These views show aligned mesenchymal cells packed along with connective tissue fibres, further connected by a tenuous yet marked fibrillary matrix that envelopes the conveyor belt in its forward mechanisms, carrying the teeth and their attachment apparatus forward along the mineralized cartilage tesserae (Fig. 9).

Figure 9

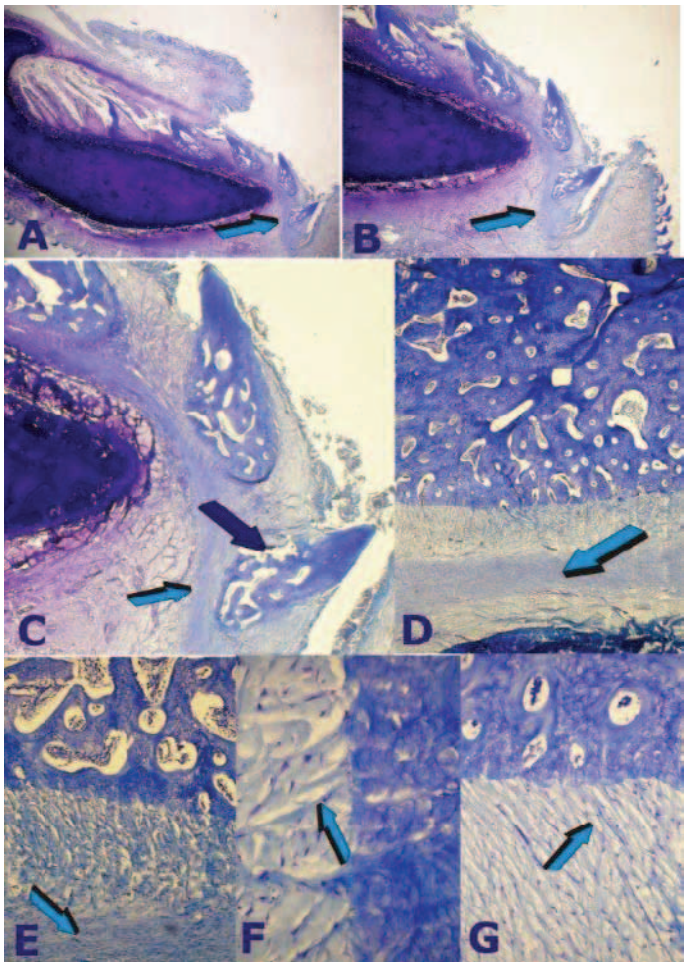

***Figure 9**. The conveyor belt mechanism, root resorption, loss of periodontal attachment, and exfoliation of more anteriorly located dental elements of the Selachian's jaw. **A**-**B**: Low power views of C. obscurus jaws depicting the rolling over movement along the cartilaginous edge of the Selachian's jaw with forward displacement of the conveyor belt (**light blue** arrows) carrying more anteriorly the teeth rolling over the edge of the jaw. **C**: The forward movement assigns the dental element into an altogether different molecular and morphogenetic micro-environment whereby episodes of dentinoclastogenesis are initiated along the surfaces of the body of the root (**dark blue** arrow in **C**) together with attachment loss that results in the exfoliation of the more anteriorly located teeth. **D**-**G**: details of the periodontal attachment apparatus of* C. obscurus. ***D**,**E**: Mesenchymal tissue relationships between the root of the teeth and the conveyor belt (**light blue** arrows). **F**,**G**: High power views of the Selachian's attachment apparatus originating from the conveyor belt and tightly inserting into the dentin-like material of the tooth surface. Note cellularity along the fibres (**light blue** arrows) almost directly inserting if not entering within the Selachian's root surface. Whole mount undecalcified sections, toluidine blue.*

It is possible that the conveyor belt is packed with myofibroblasts of Gabbiani' definition[50-52] that provide tractional forces along the connective tissue fibres, moving the teeth forward (Figs. 6,9).

Figure 10

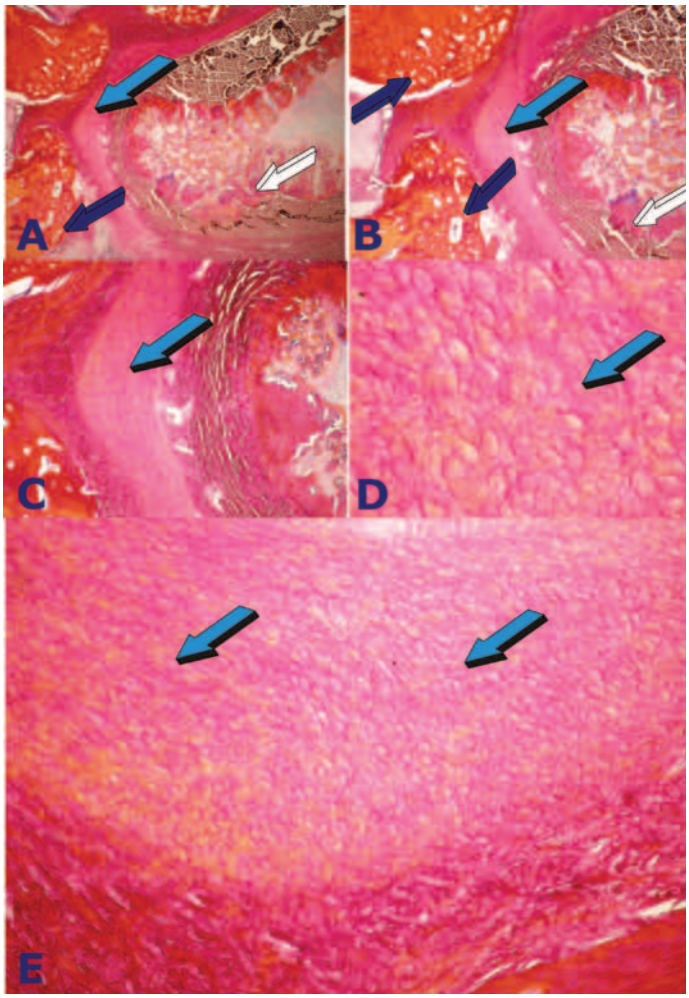

***Figure 10**. Morphology of the conveyor belt and invocated molecular mechanisms for the forward progression of the Selachian's multiple continuously erupting teeth. **A**,**B**: Low power views of* Carcharinus obscurus *anterior part of the jaw showing the mineralized tesserae (**white** arrows) with the conveyor belt' like tissue (**light blue** arrows) centrally located between the jaw and the root of the Selachian's teeth (**dark blue** arrows). **C**,**D**: High power views of the conveyor belt (**light blue** arrows) with cellular elements interspersed within the collagenous matrices (**light blue** arrow in **D**). High power view showing the conveyor' belt mechanism of tractional forces initiated by myofibroblasts of Gabbiani' definition.[51,52] Whole mount undecalcified sections, Verhoeffs' stain.*

Of note, only half of the total number of teeth are functional at any one time, the others being concealed beneath the epithelial layer. Teeth originate in the dental lamina which is a fold of the oral epithelium extending posteriorly to the lamina propria of the oral mucosa. It is the continuously erupting multiple teeth from the dental lamina within the shark's jaws that defines polyphyodonty (Figs. 5, 10,11A).

Figure 11

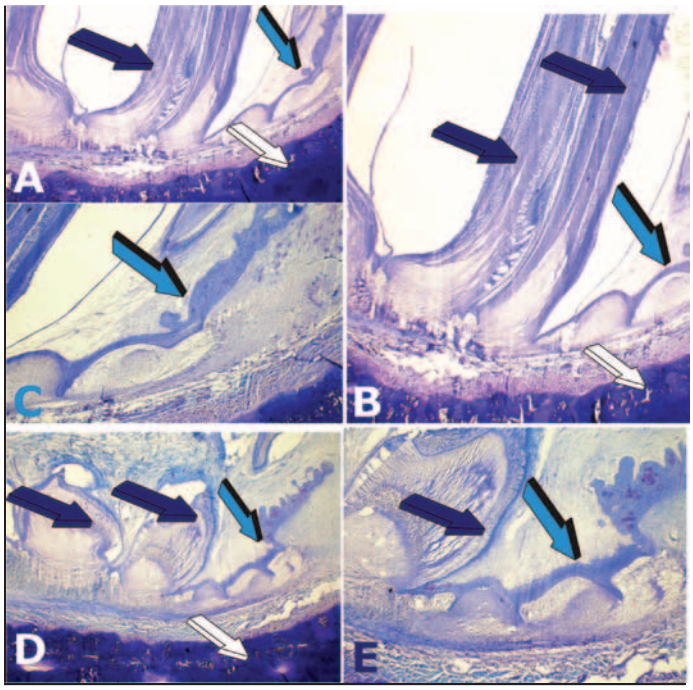

***Figure 11**. Morphological details of the continuously erupting dental lamina and forward progression of the newly formed and erupting Selachian's teeth. **A**-**C**: Developmental origin of the Selachian's teeth (**dark blue** arrows) from the continuously erupting dental lamina (**light blue** arrows) above the mineralized tesserae (**white** arrows) of the adolescent cartilaginous jaws of* Carcharinus obscurus *specimens. **D**,**E**: Morphological detail of tooth morphogenesis of the Selachian's dentition highlighting the continuously erupting dental lamina (**light blue** arrows) and the newly forming teeth (**dark blue** arrows). Undecalcified section, toluidine blue stain.*

Figure 12

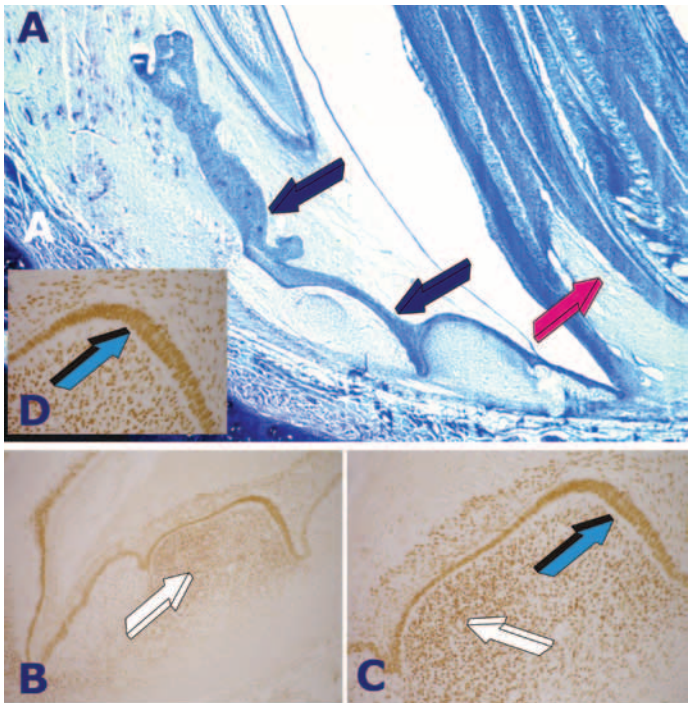

Figure 12**.* Morphological and immunolocalization studies of the continuously erupting dental lamina of Carcharinus obscurus specimens. ***A**-**C**:* Continuously erupting dental lamina *(**dark blue

arrows) yielding sequentially newly formed teeth *(**magenta** arrow)* that move forward by tractional forces of the conveyor belt *(**white** arrows).* ***B-D**:* TGF-β_3 immunolocalization of the erupting dental lamina *(**light blue** arrows)* as well as in the follicle below the erupting lamina *(**white** arrows **B,C**).* Undecalcified section, toluidine blue stain.

The dental lamina immunolocalizes the TGF-β_3 isoform (Figs. 11B,C,D), a multifunctional pleiotropic morphogen active in embryonic development in several animal phyla. It is not only localized in the dental epithelium (Fig. 11D) but also in mesenchymal proliferating cell condensations resting below the dental epithelium (Figs 11B,C) indicating further roles of the TGF-β_3 isoform in tissue morphogenesis of the *Selachian* masticatory apparatus.

Together with the cartilaginous endoskeleton and the "active skin" allowing both sinuous and powerful muscular propulsion of the shark through the waters of our oceans, the polyphydonty in *Selachian* species is the result of a natural genetic evolutionary selection that has ensured that, with no further evolution, the *Selachians* are unbeatable predators in the waters of the planet. Research has shown that tooth replacement rates are dependent on water temperatures, faster rates being recorded for summer and slower rates for winter months.

Various hypotheses have been proposed to account for the rapid tooth succession and replacements in sharks. It has been suggested that the proliferation of the dental epithelium together with the intercellular tissue fluid tension cause the forward movement of the *Selachian*'s teeth.[54] One opinion held that fluid pressure within vacuoles situated in the tissue layer below the tooth bands create the forces necessary for tooth movement.[54] It has been suggested that the expansion of the jaw cartilage during growth may account for tooth replacement. However, the cartilage expands only during growth and development, whereas continuous tooth replacement occurs throughout the life of the *Selachian* fishes.

Shark teeth consist mainly of dentine, (variously termed *enameloid*, *mesodermal enamel* or *durodentin*) covered with a calcified layer of ectodermal enamel, which is derived from ameloblastic activity and is attached to the underlying epithelial tissues by means of basal calcified tissue.[20] This enameloid covering of the tooth crown corresponds to the mammalian tooth enamel.[54] Moss claims that bone is present at the base or pedicle of shark teeth and placoid scales.[20]

Researchers in 1979, conducting a histological study on the jaws of three shark species, observed that between the teeth and the tesserae layer of the jaw there are two layers of dense connective tissue.[48] The upper layer is the tooth bed which contains large collagen fibres that radiate into the calcified matrix of the jaws. These fibres are akin to the Sharpey's fibres seen in the mammalian periodontium,[54] and serve as anchorage for the tooth. The inner layer (or supra-tesseral layer) of connective tissue is similar, also having Sharpey-like fibres but with anchorage into the outer layer (or cap) of the tesserae. There are blood vessels between these two connective tissue layers but very few branches are directed toward the tesserae.

The *Selachian*'s attachment apparatus, then, is composed of several fibres uniting the conveyor belt to the root surfaces in the tridimensional space embedded within the supra-belt connective tissue (Fig. 9D, E). More coronally, connective tissue fibres, resembling periodontal ligament fibres as seen in mammals, connect the root surfaces to the surrounding mesenchymal tissues of the *Selachian*'s root microenvironment (Figs. 9F,G).

A distinctive feature in sharks, as opposed to mammals, is that, more medially or anteriorly along the cartilaginous jaw, which is reinforced by mineralized tesserae, there is connective tissue attachment loss together with dentinoclastogenesis that eventually results in the exfoliation of teeth. Lost teeth are replaced by new rows of teeth which have been transported along the conveyor belt (Fig. 9). We have envisaged mechanical tractional forces set into motion by the mechano-transduction activity of the myofibroblasts[50,51] that effectively transport the *Selachian*'s' dentition forward, (Fig 4) replacing rows upon rows of exfoliated teeth.

The mechano-transducer conveyor belt also plays a fundamental role in tooth replacement. Low power digital images of the *Selachian*'s jaws show that when the edge of the cartilaginous jaw is reached, the connective tissue belt moves further anteriorly to the profile of the jaw, together with the teeth and their tractional bundle of connective tissue (Figs.9A,B,C). The more anterior region is thus anatomically different and occupies a different molecular microenvironment whereby root resorption is set in train after activation of dentinoclasts (Fig. 9C).

Vertebral centra (Fig. 7) were first used for assessing age in *Elasmobranchs*; growth bands of shark centra were visualized by fluorescent markers to assess age and growth of leopard sharks *Triakis semifasciata*. An examination of the vertebrae of seven elasmobranch species found that *Carcharhinids* had the strongest vertebral centra, and that *Elasmobranch* vertebral cartilage is comparable in ultimate strength to mammalian bone.[45] Mineralization in the jaws is related to their individual mineralized subunits, i.e. tesserae along the border of the cartilaginous matrix.

Carcharinus obscurus or dusky shark species are found in the Atlantic, Pacific and Indian Oceans and can measure up to four meters in length. Dusky sharks are long-lived (up to 40 years of age) reaching sexual maturity at approximately 20 years of age. They give viviparous birth to offspring that measure between 85 and 100 cm. The maxillary teeth of *C. obscurus* are triangular and slightly oblique; the mandibular teeth are erect with narrow cusps. Dermal denticles (placoid scales) cover the integument of *C. obscurus* and are large and closely imbricated (Fig. 8).

- Studies have reported signs of an osteogenic programme during tissue morphogenesis in selected *Elasmobranch* species,[55,56] further supporting the concept of the bony origin of the exoskeletal tissues of dermal denticles. The possibility of "forcing" and/or "reprogramming" the induction of bone formation in shark intramuscular heterotopic sites became feasible as a result of the simultaneous availability of several key factors :
- The extraction and purification of vertebral and chondrocranial proteinaceous material,
- large doses of recombinant human osteogenic proteins-1 (hOP-1),
- highly purified naturally-derived bone morphogenetic protein fractions, then labelled as osteogenin,[9]
- the contemporary use of macroporous self-inducing coral-derived constructs.[12,13]

In addition, *in vivo* bioassay studies were undertaken to find out whether shark cartilage extracts might have retained osteoinductive proteins which could induce heterotopic bone formation in both the rodent and shark.

Shark tissue harvest and preparation of cartilaginous vertebrae and chondrocrania for protein extraction and purification.

Overall, the study encompasses a period from 1989 to 1994. The last bioassay of the intramuscular heterotopic sites of captive *C. obscurus* was completed in February 1994 at the Oceanographic Research Institute, Marine Parade, Durban, where captive sharks were housed. Records of the prolonged experimentation, including the rationales, material, methods, procedures and results were kept in two NIH record books 7530-00-222-3525. Federal Supply Service dated 1989 and 1990. The work fluctuated from the South African shores at Umhlanga Rocks, to the Dental Research Institute and later at the Bone Research Laboratory, Johannesburg, to the US shores at the National Institutes of Health, Bethesda, Bone Cell Biology Section, back again to the Bone Research Laboratory and finally again to the Oceanographic Research Institute to harvest the last heterotopically implanted *C. obscurus* animals.[53]

From June 1989 up to May 1990, with the help of the Natal Shark Board Umhlanga, sixteen *C. obscurus* and one *C. taurus* were harvested off the Indian Ocean. Animals brought to the decks of the boats were euthanized with 7 to 12 ml sodium pentobarbitone injected through the ampulla in the cephalic ventral area. Whilst we were still at sea and fishing for additional adolescent *C. obscurus*, euthanized animals were dissected so as to efficiently harvest vertebral and chondrocranial cartilage material; jaws were dissected free and used only for histology and morphological analyses after fixation in 70% ethanol. Cartilages were kept on ice below board.

The harvested vertebrae and chondrocrania were cleansed of all the attached connective tissue as best as possible. When in the laboratories, the harvested cartilage was cooled with liquid nitrogen and immediately wrapped in cotton cloth and placed on the laboratory benches. Cartilages were frantumated (shattered) and partly pulverized using a rubber hammer. The samples were dehydrated in ethanol and ethyl ether yielding a total of 934.12 g of vertebrae cartilaginous material; the corresponding chondrocranial material amounted to 429.4 g. Batches of cartilage harvested from *C. taurus* were extracted and partially purified at the Dental Research Institute of the University whilst the bulk of the dehydrated vertebrae and chondrocrania underwent extraction and the resulting proteins partially purified at the Bone Cell Biology Section, NIH, Bethesda, USA, July/August 1990.[53]

Chaotropic extraction of cartilaginous vertebrae and chondrocrania

Batches of dehydrated cartilage of both vertebrae and chondrocrania were demineralized with 10 volumes of 0.1N hydrochloric acid (HCl) under continuous monitoring of the pH to measure available hydroxyapatite ions. Cartilage batches were deemed demineralized after the fourth wash showed a constant strongly acid pH. The demineralized cartilage was then washed with deionized water to restore neutrality.

Different batches of approximately 200/300 g each were extracted with 4l 1,2 M guanidinium hydrochloride (Gdn-HCl) with enzyme inhibitors (ε-amino caproic acid, benzamidine, and phenil methyl sulphonyl fluoride (PMSF), performed overnight in the cold with 20 g Ultrol®Grade Chaps {3-[(3-cholamidopropyl}-dimethylammonio-1-propanesulfate}. The supernatant was drained off and centrifuged for 3hrs at 3000 rpm to remove proteoglycans. Vertebrae and chondrocrania were re-extracted with 1,2 M Gdn-HCl 0,5M acetic acid, pH 3,0 with enzyme inhibitors as above to further slightly demineralize the re-extracted residue.

Vertebrae (and chondrocrania in separate experiments) were re-homogenized with short bursts of a polytron homogenizer. Extracts, kept cold all the times, were concentrated using a Pharmacia Filtron Ultrafiltration Unit. Extracts were diluted with 6l 0,5M acetic acid passed through an Amicon YM-100 spiral ultrafiltration cartridge to remove proteins having molecular weights higher than 100kD. The recovered proteins, of less than 100kD, were concentrated using the Pharmacia Filtron ultrafiltration unit (8l > 500ml – add 3,5l Urea = 7 volumes) to a final concentration of 500 ml 6M Urea/50mM Tris, pH 7.4.

Purification of vertebraL and chondrocraniaL extracts, Heparin-Sepharose and Hydroxyapatite -Utrogel affinity and adsorption chromatography.

After concentration and exchange to 6M urea/50MmM Tris, pH 7.4, the extracts were loaded onto hydroxyapatite Ultrogel adsorption chromatography. eluted with 100 mM Na/Phosphate. Concentrated and exchanged eluates were loaded onto a heparin-Sepharose affinity chromatography column with a modified affinity column for further interactions between extracts and the chromatography gel. A 500ml Heparin-Sepharose gel was added to a 2l container and washed twice with 500 ml 6M Urea/0.50mM NaCl, 50mM Tris, pH 7.4. Cartilage extracts were then added adjusting the salt concentration to 0.15M NaCl by adding dry NaCl. The gel was mixed overnight under continuous stirring in the cold. The Heparin- Sepharose gel and bound fractions were repacked into a Pharmacia 500ml column and left to settle for at least an hour. The column was then washed with two column volumes of 0.15M NaCl, 6M Urea, 50mM Tris to wash off the unbound proteins. The column was then eluted with 6M Urea/50mM Tris, 1M NaCl, pH 7.4.

Characterization of protein extracts, preparation of protein samples for bioassay in rodents.

The 1M NaCl 6M Urea/50mM Tris eluates after affinity chromatography of vertebral and/or chondrocranial extracts were concentrated to 150ml and exchanged to 4M Gdn-HCl/50 mM Tris and to final concentrations of 7 to 21ml 4M Gdn-HCl/50 mM Tris, pH 7.4. Seven to twenty-one ml of eluate of protein concentrates after Heparin-Sepharose affinity chromatography from either vertebrae or chondrocrania were loaded onto tandem Sephacryl S-200 HR (high resolution, Pharmacia) gel filtration chromatography columns, equilibrated and eluted as described.[9,28] Two ml aliquots from tubes 21 to 31 were concentrated in centricons to ~200µl. 100µl of concentrate sample was used for reconstitution and bioassay in heterotopic sites of Long-Evans rats. Protein concentrations ranged from 175 to 540µg (vertebral extracts) and from 107 to 266 µg (chondrocranial extracts). Proteins were added to 25mg of insoluble collagenous bone matrix of Long-Evans rat suitably prepared.[9,28] Two lyophilized pellets were implanted subcutaneously bilaterally under the skin of the chest of each rat [9,28] for a total of 22 implants in 11 Long-Evans rats.

Implantation of cartilaginous extracts and bone morphogenetic proteins in vivo *in heterotopic intramuscular sites of* Carcharinus obscurus.

A total of nine adolescent *Carcharinus obscurus* ± 120cm in length were captured on different occasions at Umhlanga Rocks, north of Durban, South Africa. Animals were rapidly brought to the Oceanographic Research Institute by the Natal Shark Board fast boats and housed in the facilities of the Research Institute, Marine Parade, Durban. In three pre-planned surgical proce-

dures – cleared by the Animal Ethics Committee of the University of the Witwatersrand, Johannesburg – general anaesthesia was induced with ketamine-HCl. Operating at the edge of the salty ponds of the Institute the anaesthetized animals were implanted with one to four implants per animals. Time constraints had been stipulated by the Animal Ethics Screening Committee of the University so that in some animals no more than one or two pellets of osteogenic material were implanted. After incisional wounds and blunt dissection of the muscular tissue, lyophilized implants were inserted within the muscle pouch.

Table I below reports the number of implants and the type of implanted material after reconstitution with either vertebral or chondrocranial extracts, naturally-derived highly purified bone morphogenetic proteins,9 as well as recombinant human osteogenic protein-1 (hOP-1) delivered by either the extracted cartilaginous residues, synthetic RG503 matrix or by coral-derived fully-converted hydroxyapatite constructs with and without BMPs or hOP-1 as control.

Proteins concentrations of the different extracts and level of purification varied considerably across the purification scheme, from 4.15 to 7.76 mg/ml in crude extracts from both vertebrae and chondrocrania, to 0.82 mg/ml in Hep 1M fractions down to 540 to 175 or 266 to 107 µg as evaluated in S-200 gel filtration fractions from both vertebral and chondrocranial protein fractions eluates.

Table 1. Number of implanted specimens and type of osteogenic inductive morphogens reconstituted with various delivery systems as carrier for osteoinduction

Osteoinductive Morphogen(s)	Number of implants	Number of Carcharinus obscurus	Time of tissue harvest
0.5 & 2.5 mg hOP-1 in RG503 matrix	6	A total of 17 C. obscurus housed at the Oceanographic Research Institute were used to implant 27 different osteogenic preparations as discussed in text. Animals were implanted with one to four implants each (see text)	21 and 37 days
Naturally-derived osteogenin + shark residue	2		21 days
S-200 shark vertebrae extracts	3		21 days
S-200 shark chondrocrania extracts.	4		21 days
shark residue control	4		21 and 37 days
Coral-derived construct control	3		21 and 37 days
Coral-derived constructs + hOP-1 in RG503	3		21 and 37 days
	3		21 days

Key : hOP1: osteogenic protein-1; RG503 synthetic matrix as carrier for hOP-1; S-200: gel filtration fractions after Sephacryl S-200 gel filtration chromatography; coral-derived construct: coral-derived macroporous hydroxyapatite after full hydrothermal conversion of calcium carbonate into hydroxyapatite.

Histological evaluation of tissue induction after in vivo *implantation of cartilaginous extracts and bone morphogenetic proteins in heterotopic intramuscular sites of rodents.*

Various extracts and purified protein fractions from either chondrocranial or vertebral cartilaginous matrices purified by gel filtration chromatography were reconstituted with allogeneic rat insoluble collagenous bone matrix residue and implanted in the subcutaneous space of the chest bilaterally in Long-Evans rats.

Tissue sections prepared from specimens harvested on day 12 after heterotopic implantation showed the invasion of multiple cellular elements between the allogeneic collagenous matrix particles with several rounded nuclear cells together with multinucleated giant cells with overall limited vascular invasion and angiogenesis (not shown). No cartilage or bone induction was observed in any of the examined sections (not shown).

Figure 13

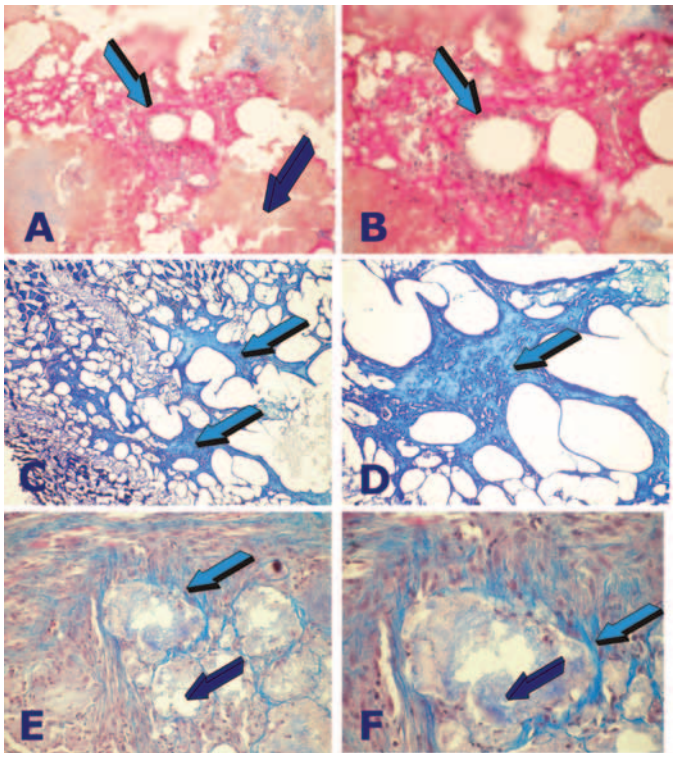

***Figure 13**. Bioassay of morphogenetic soluble signals partially purified after liquid chromatography of extracts of vertebrae and/*

or chondrocrania of the Selachians and tissue induction by recombinant human osteogenic protein-1 (hOP-1) implanted intramuscularly with carrier matrices in *C. obscurus*. ***A***,***B*** Morphogenetic inductive gradients induced by) 0.5 mg hOP-1 combined with the synthetic RG503 polymeric carrier. Tissue induction of a calcified matrix with lacunae surfaced by cellular elements highly reminiscent of lamellar/osteonic bone *(**light blue** arrows).* ***C***,***D****: Induction of mineralized matrix (**light blue** arrows)* by 2.5 mg hOP-1 with multi-cellular lacunae highly suggestive of osteocyte lacunae but lack of cellular elements surfacing the newly formed tissue within the selachian's mucle. ***E***,***F***: Reconstitution of 0.5 mg hOP-1 with synthetic RG503 polymeric carrier (dark blue arrows - color bold TY) induces cellular and matrix tissue formation surrounding the implanted carrier *(**light blue** arrows)* highly reminiscent of the induction of bone formation with however lack of osteoblastic-like cells differentiation.

Specimens of rat allogeneic bone matrix reconstituted with 3 µg recombinant human osteogenic protein-1 (hOP-1) as positive control, induced cartilage and bone differentiation in heterotopic subcutaneous sites in the rodent bioassay (not shown).

Morphological and histological evaluation of tissue induction after in vivo implantation of cartilaginous extracts and bone morphogenetic proteins in heterotopic intramuscular sites of Carcharinus obscurus *sharks.*

Several inductive preparations delivered by either cartilaginous shark residue or coral-derived macroporous bioreactors as well as synthetic matrices were implanted in heterotopic intramuscular pouches created by sharp and blunt dissections in several recipient *C. obscurus* adolescent sharks.

Figure 13 shows tissue induction upon delivery of 0.5 or 2.5 mg recombinant hOP-1 in RG503 synthetic matrix implanted intramuscularly in *C. obscurus* and harvested on day 21 after heterotopic implantation. Tissue induction resulted in deposition of mineralized matrix resembling bone matrix with osteonic structures covered by cellular elements secreting the matrices, possibly pseudo-osteoblasts-like cells palisading the newly secreted matrices (Figs.13A,B).

Additional specimens representing heterotopic sites implanted with the higher dose of hOP-1 (2.5 mg recombinant hOP-1 in RG503 synthetic matrix) also showed the induction of mineralized trabecular-like tissue but without evidence of cellular elements along the trabecular surfaces (Figs. 13C,D).

High power view of heterotopically implanted specimens of 0.5 mg hOP-1 in RG503 synthetic matrix showed the induction of extracellular deposition with cellular activities within the matrix surrounding the implanted synthetic RG503 matrix (Figs. 13E,F). RG503 matrix without hOP-1 showed fragmentation of the synthetic carrier within the muscular tissue (not shown).

Specimens of collagenous residues recombined with S-200 fractions from either chondrocrania and/or vertebrae extracts showed encapsulation without evidence of chondrogenesis and/or osteogenesis (not shown).

Some tissue specimens could not be identified, being either totally absorbed or damaged by the shark movements after implantation; only one relatively intact specimen of coral-derived macroporous bioreactor could be identified and thoroughly processed; other coral-derived constructs presented as crushed and, although histologically processed, tissue invasion and/or induction within the macroporous spaces could not be easily identified.

It is noteworthy that a coral-derived macroporous construct implanted as control without addition of naturally-purified osteogenin and/or recombinant hOP-1 showed a significant chondrogenic tissue induction within the macroporous spaces (Fig. 13).

Figure 14

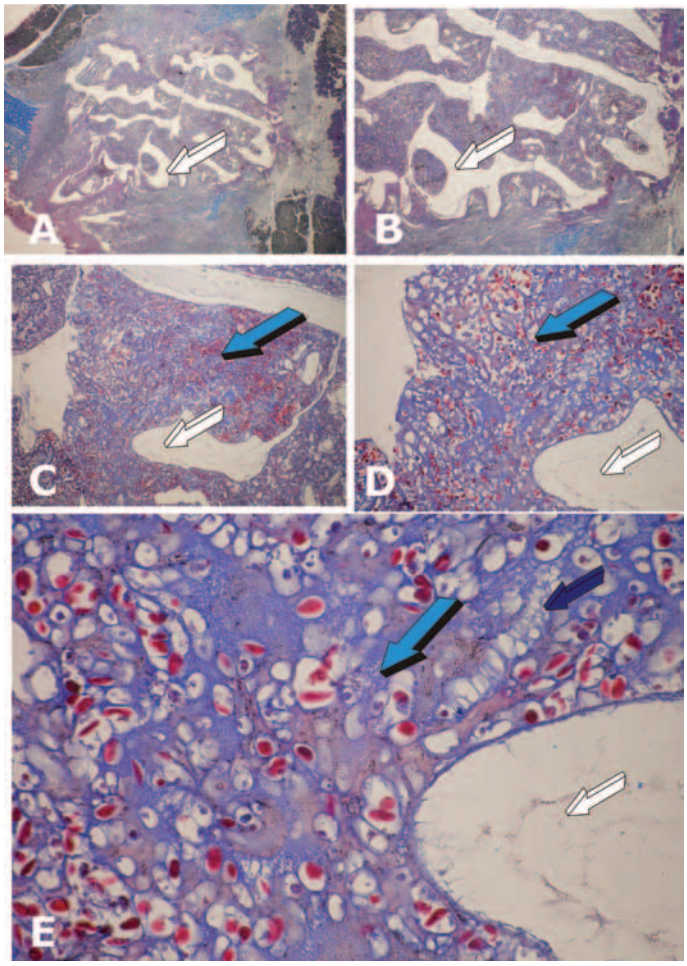

Figure 14*. Within the limit of the implantation constraints into the intramuscular sites of the Selachian's tissues at the Oceanographic Research Institute, Marine Parade, Durban, we were able to implant a number of coral-derived macroporous calcium-carbonate/hydroxyapatite bioreactors in heterotopic sites of the muscle tissues of selected sharks. The bioreactors were pre-loaded with recombinant human osteogenic protein-1 (hOP-1), highly purified naturally- derived osteogenic protein fractions (osteogenin.*[9] *and hOP-1 pre-combined with RG503 synthetic matrices. Macroporous constructs were also implanted* solo *as control. Because of the inherent fragility of the calcium/phosphate constructs several specimens could not be properly retrieved or the histology showed only the crumpled aspect of the implanted bioreactors. One control specimen was amenable to proper histological processing and sectioning with successful staining of the newly formed induced tissues developing within the macroporous spaces.* ***A***,***B****: Low power views of the implanted constructs (**white** arrows).* ***C***,***D****: Induction of tissue formation within the macroporous spaces (**light blue** arrows) of cartilage-like material.* ***E****: Induction of cartilage with secretion of cartilaginous matrices (**light blue** arrow). Note columns of progressively differentiating chon-*

*droblasts (**dark blue** arrow) patterning the newly formed cartilage as in mammalian embryonic development. We speculate that the micro-inductive micro-environment of the coral-derived macroporous bioreactors engineers cartilaginous columnar condensations as seen in the mammalian counterpart. Tissue induction however lacks the induction of bone differentiation. The absence of an inductive programme setting into motion the induction of bone formation is possibly due to the evolutionary lack of genes regulating the bone induction cascade; alternatively, we do believe that the lack of vascular invasion followed by chondrolysis may be responsible for the lack of bone formation after evolutionary expression and synthesis of powerful inhibitors of angiogenesis (see text for detail) that block osteogenesis in angiogenesis.* [10,11,15]

Chondrogenesis developed within the macroporous spaces even without the exogenously application of osteogenic morphogens (Fig. 14). Differentiated chondrocytes showed the secretion of chondrogenic extracellular matrix within the macroporous spaces and were thus embedded within the secreted matrix (Fig. 14E).

DISCUSSION, COMMENTS AND PERSPECTIVES

The study explored several biochemical and tissue induction phenomena in different animal species under the vast and pleiotropic umbrella of tissue induction and tissue biology by an array of morphogenetic substances with a vast pleiotropic cascade of biological activities. Certainly, the most salient result of the reported multiple studies is the induction of chondrogenesis by the heterotopically implanted coral-derived macroporous bioreactor.

Selected points should be discussed as novel information of the biology of the *Selachian*s. The identification of a clear cut conveyor belt *via* special stains that moves the newly formed set of teeth forward by the continuously erupting dental lamina is worthwhile, and hence our hypothesis that such forward movement is controlled by modified myofibroblasts of Gabbiani's definition.[50-52] This molecular tractional pathway needs further explorative research by selected immunohistochemistry. A recent molecular and morphological investigation did report the presence of specific genes that govern the development and continuous regeneration of teeth in sharks.[59]

The immunolocalization of the TGF-β_3 protein within the tesserae of the jaws and in the proliferating epithelium is of great significance, and additionally indicates that *Selachian* tissues do retain morphogens that in primates are powerfully inducers of endochondral bone formation.[38-40]

The TGF-β_3 immunolocalization in the continuously erupting dental lamina is also noteworthy and suggests that the pleiotropic morphogen is also biologically active in the induction of tissue morphogenesis in *Selachian* tissues. A recent contribution, appearing in *Bone,* has indicated that TGF-β_2 signalling is essential for osteoblast migration and differentiation in the medaka fish.[58] *In situ* hybridization has shown the importance of TGF-β_2 expression during fracture healing of the medaka fish. However, this is a bony fish. In *Selachian*s, there is no bone, yet immunolocalization has shown the expression of the TGF-β_3 isoform. This indicates – as often previously stated - the ancient signalling pathways shared by several genera and species across the induction of tissue morphogenesis, from the fruit fly *Drosophila melanogaster*, to the bony fish medaka, to the non-human primate *Papio ursinus* to the human primate *Homo sapiens*, back to the amphibian tongueless and toothless African clawed toad *Xenopus laevis*.

Finally, and perhaps most importantly, a coral-derived construct without any adsorption of exogenously applied morphogenetic inductive signals, has activated the induction and differentiation of cartilage tissue within the heterotopically implanted macroporous spaces. As we have recently reported in *Biomaterials*:[32] "*the unique connubium of the hydrothermally exchanged coral-derived bioreactors, Ca^{++} release, angiogenesis, stem cell differentiation with expression and secretion of both angiogenic and osteogenic soluble molecular signals sets into motion the construction of the morphogenetic gradient of the macroporous bioreactor. Spontaneously, the bioreactor thus initiates the induction of bone formation even without the exogenous application of the osteogenic soluble molecular signals of the TGF-β supergene family*".

We thus report in our final statement that in heterotopic intramuscular sites in *Selachian*s, the coral derived bioreactor does not initiate the cascade of bone differentiation but rather the induction of chondrogenesis within the macroporous spaces. The DNA of the *Selachian*s does not have the developmental memory of the osteoinduction programme though it retains the induction of chondrogenesis as a recapitulation of evolutionary differentiating and de- differentiating events, ultimately lacking the angiogenesis and capillary sprouting required for setting chondrolysis into motion Thus it may not restore the extinct signalling pathways of the induction of bone formation.

ACKNOWLEDGMENTS

The experiments on shark cartilages, harvesting the *Selachian* fishes out of the green waters of the Indian Ocean, the harvesting of the *Selachian* cartilages on the rolling decks of the powerful boats of the Natal Shark Board, working at the Dental Research Institute and later at the Bone Cell Biology Section of the NIH in the USA, flying back to Africa to implant not only purified shark extracts but recombinant human bone morphogenetic proteins intramuscularly in sharks together with purifying baboon osteogenin to homogeneity at the NIH has excited us to no end and determined our scientific performance and our hard and multiple tasks for several years ahead. The NIH period was for all of us the beginning of a scientific intellectually fascinating ride across the vast phenomena of the induction of bone formation, the spontaneous inductivity, animal phyla, molecular evolution, speciation and de-differentiation. We thank Hari Reddi, presently distinguished Professor and Hellison Chair, Musculoskeletal Molecular Biology, Centre for Tissue Regeneration and Repair, the University of California, Davis, USA, who made available to us back in the nineties his mind and his laboratories, not only to purify baboon bone matrices but also shark cartilages. We wish to thank Frank Luyten, then associate researcher with AH Reddi at the Bone Cell Biology Section for his help and suggestions on the shark cartilage extraction and purification. A note of thanks to Shabnum Meer, Oral Pathology, University of the Witwatersrand, Johannesburg, for discussing and diagnosing cartilage induction as reported in Figure 14. Preparing a manuscript with significant information and digital iconography and remaining continuously in touch with co-authors and the Bone Research Unit at the University entails communication often difficult when overseas. For the use of the IT connection, paper, printers – colour and black and white – the senior author would like to thank Carlo Brambilla and his outstanding wireless connection in Carnate, Milano, Francesco of the Sangiorgio Calzature, Merate, Milano, and finally Alberto and his team of managers at the Spar Mountain Lake, Broederstroom, North West Province, South Africa. This critical help as well as interest have been fundamental for many papers conceived, prepared and published by the Bone Research Laboratory of the University.

DECLARATION: There is no conflict of interest.

References

1. Cousteau V. How to swim with sharks. Perspective in Biology and Medicine 1987; 30: 486-9.
2. Editor's Note In Voltaire Costeau: How to swim with sharks. Perspectives in Biology and Medicine 1987; 30:486-89.
3. Mathews MB. The molecular evolution of cartilage. Clin Orthop Relat Res 1966; 48:26783.
4. Grady JE. Tooth development in sharks. Archs Oral Biol 1970 ;15: 613-9.
5. Venkatesh B, Lee AP, Ravi V, Maurya AK, Lian MM, Swann JB, et al. Elephant shark genome provides unique insights into gnathostome evolution. Nature 2014; 505:174-9.
6. Romer A. The ancient history of bone. Ann NY Acad Sci, 1963;109: 168-73.
7. Stensiö EA. The downtonian and Devonian vertebrates of Spitzbergen. Pt I: Family Cephalaspidae Skr Svalb Nordish 1927; 12: 1-391.
8. Trueta J. The role of the vessels in osteogenesis. J Bone Joint Surg 1963 ;45-B: 402-18. 48. Baylink D, Wergedal J, Thompson E. Loss of proteinpolysaccharides at sites where bone mineralization is initiated. J Histochem Cytochem 1972;20: 279-92.
9. Ripamonti U, Ma S, Cunningham NS, Yeates L, Reddi AH.) Initiation of bone regeneration in adult baboons by osteogenin, a bone morphogenetic protein. Matrix 1992;12:369-80.
10. Ripamonti U, Ferretti C, Heliotis M. Soluble and insoluble signals and the induction of bone formation: Molecular therapeutics recapitulating development. J Anat 2006; 209:447-68.
11. Ripamonti U. Soluble osteogenic molecular signals and the induction of bone formation. Biomaterials 2006; 27: 807-22.
12. Ripamonti U. The morphogenesis of bone in replicas of porous hydroxyapatite obtained from conversion of calcium carbonate exoskeletons of coral. J Bone Joint Surg Am1991: 73(5: 692-703.
13. Ripamonti U, van den Heever B, Van Wyk J. Expression of the osteogenic phenotype in porous hydroxyapatite implanted extraskeletally in baboons. Matrix 1993; 13:491-502.
14. Ripamonti U, Ramoshebi LN, Patton J, Matsaba T, Teare J, Renton L. Soluble signals and insoluble substrata: Novel molecular cues instructing the induction of bone. In EJ Massaro and JM Rogers (Eds.), Chapter 15, The Skeleton, Humana Press, 200: pp 217-27.
15. Ripamonti U, Heliotis M, Ferretti C. Bone morphogenetic proteins and the induction of bone formation: From laboratory to patients. Oral and Maxillofac Surg Clin North Am 2007; 19:575-89.
16. Ripamonti U, Klar RM. Redundancy of osteogenic molecular signals initiating the induction of bone formation. Science in Africa 2010. http://www.scienceinafrica.co.za/2010/october/bone_regeneration_full.htm
17. Crivellato E, Nico B, Ribatti D. Contribution of endothelial cells to organogenesis: A modern reappraisal of an old Aristotelian concept. J Anat 2007; 211:415-27.
18. Ripamonti U. *Quo vadis* Bone Regeneration – Feature paper – Science in Africa November 2010
19. Kusumbe AP, Ramasamy S, Adams RH. Coupling of angiogenesis and osteogenesis by a specific vessel subtype in bone. Nature 2014; 507:323-8.
20. Moss ML. Skeletal tissues in sharks. Amer Zool 1977 ; 17: 335-42.
21. Langer R, Brem H, Falterman K, Klein M, Folkman J. Isolation of a cartilage factor that inhibits tumor neovascularization. Science 1976 ; 193:70-2.
22. Moses MA, Sudhalter J, Langer R. Identification of an inhibitor of neovascularization from cartilage. Science 1990; 248: 1408-10.
23. Lee A, Langer R. Shark cartilage contains inhibitors of tumor angiogenesis. Science 1983; 221: 1185-7.
24. Moses MA, Langer R. Inhibitors of angiogenesis. Biotechnology 1991; 630-5.
25. Turing AM. The chemical basis of morphogenesis. Philos Trans Roy Soc Lond 1952;237:37-49.
26. Lacroix P. Les mécanismes élémentaires de l'ossification endochondrale. Arch Biol(Liege) 194;) 56: 351-82.
27. Sampath TK, Muthukumaran N, Reddi AH. Isolation of osteogenin, an extracellular matrix-associated, bone-inductive protein, by heparin affinity chromatography. Proc Natl Acad Sci USA 1987;84:7109-13.
28. Luyten FP, Cunningham N S, Ma S, Muthukumaran N, Hammonds RG, Nevins WB, Woods WI, Reddi, AH. Purification and partial amino acid sequence of osteogenin, a protein initiating bone differentiation. J Biol Chem 1989; 264:13377-80.
29. Urist MR. Bone: Formation by autoinduction. Science 1965; 150:893-899.
30. Sampath TK, Reddi AH. Dissociative extraction and reconstitution of extracellular matrix components involved in local bone differentiation. Proc Natl Acad Sci USA 1981; 78: 7599-603.
31. Sampath TK, Reddi AH. Homology of bone-inductive proteins from human, monkey, bovine, and rat extracellular matrix. Proc Natl Acad Sci USA 1983; 80: 6591-5.
32. Ripamonti U, Roden LC, Renton LF. Osteoinductive hydroxyapatite-coated titanium implants. Biomaterials 2012; 33:3813-3823.
33. Ripamonti U. Tissue engineering of bone by novel substrata instructing gene expression during *de novo* bone formation. Science in Africa 2002. http://www.scienceinafrica.co.za/2002/march/bone2.htm
34. Ripamonti U, Klar RM. Redundancy of osteogenic molecular signals initiating the induction of bone formation. Science in Africa 2010: http://www.scienceinafrica.co.za/2010/october/bone_regeneration full.htm
35. Ripamonti U, Dix-Peek T, Parak R, Milner B, Duarte R. Profiling bone morphogenetic proteins and transforming growth factor-βs by hTGF-β3 pre-treated coral-derived macroporous constructs: The power of one. Biomaterials 2015; 49:90-102.
36. Ripamonti U, Ferretti C. Mandibular reconstruction using naturally-derived bone morphogenetic proteins: A clinical trial report. In: TS Lindholm (Ed.), Advances in Skeletal Reconstruction Using Bone Morphogenetic Proteins 2002: World Scientific Publ. Co. Singapore; pp 277-89.
37. Ferretti C, Ripamonti U. Human segmental mandibular defects treated with naturally- derived bone morphogenetic proteins. J Craniofac Surg 2002; 13: 434-44.
38. Klar M R, Duarte R, Dix-Peek T, Ripamonti U. The induction of bone formation by the recombinant human transforming growth factor-β3. Biomaterials 2014; 35: 2773-88 http://dx.doi.org/10.1016/j.biomaterials.2013.12.062
39. Ripamonti U, Duneas N, van den Heever B, Bosch C, Crooks J. Recombinant transforming growth factor-β_1 induces endochondral bone in the baboon and synergizes with recombinant osteogenic protein-1 (bone morphogenetic protein-7) to initiate rapid bone formation. J Bone Miner Res 1997; 12:1584-95.
40. Ripamonti U, Ramoshebi LN, Teare J, Renton L, Ferretti C. The induction of endochondral bone formation by transforming growth factor-β3: Experimental studies in the non-human primate *Papio ursinus*. J Cell Mol Med 2008; 12: 1029-48.
41. Ifft JD, Zinn DJ. Tooth succession in the smooth dogfish, *Mustelus canis*. Biol Bull 1948;95, :100-6.
42. Martin AP, Naylor GJ, Palumbi SR. Rates of mitochondrial DNA evolution in sharks are slow compared with mammals. Nature 1992; 357: 153-5.
43. Urist MR. Calcium and phosphorus in the blood and skeleton of the Elasmobranchii. Endocrinology 1961;69: 778-801.
44. Dingerkus G, Séret B, Guikbert E. Multiple prismatic calcium phosphate layers in the jaws of present-day sharks (Chondrichthyes; Selachii). Experientia 1991;47: 38-40.
45. Porter ME, Beltrán JL, Koob TJ, Summers AP. Material properties and biochemical composition of mineralized vertebral cartilage in seven elasmobranch species (*Chondrichthyes*). J Exp Biol 2006 ; 209: 2920-8.
46. Gelsleichter JJ, Musick JA, Van Veld P. Proteoglycans from the vertebral cartilage of the clearnose skate, *Raja eglanteria*: Inhibition of hydroxyapatite formation. Fish Physiol Biochem 1995; 14: 247-51.
47. Baylink D, Wergedal J, Thompson E. Loss of proteinpolysaccharides at sites where bone mineralization is initiated. J Histochem Cytochem 1972;20: 279-92.
48. Kemp NE, Westrin SK.) Ultrastructure of calcified cartilage in the endoskeletal tesserae of sharks. J Morphol 1979;160: 75-109.
49. Dean MN, Summers AP. Mineralized cartilage in the skeleton of chondrichthyan fishes. Zoology 2006; 106:164-8.

50. Gabbiani G. Presence of modified fibroblasts in granulation tissue and their possible role in wound contraction. Experiential 1971; 15:549-550.
51. Gabbiani G. The myofibroblast in wound healing and fibro-contractive diseases. J Pathol 2003; 200: 500-3.
52. Hinz B, Phan SH, Thannickal VJ, Galli A, Bochaton-Piallat M-L, Gabbiani G. The myofibroblast – one function, multiple origins. The Am J Path 2007; 170: 1807-16.
53. Yeates B and Ripamonti U. NIH Record Book 1990.
54. Reif WE. Development of dentition and dermal skeleton in embryonic *Scyliorhinus canicula*. J Morphol 1980; 166:275-88.
55. Boyde A, Jones SJ. Scanning electron microscopy of cementum and Sharpey fibre bone. Z Zellforsch Mikrosk Anat 1968; 92:536-48.
56. Eames BF, Allen N, Young J, Kaplan A, Helms JA, Schneider RA. Skeletogenesis in the swell shark *Cephaloscyllium ventriosum*. J Anat 2007; 210: 542-54
57. Sasagawa I. Mineralization patterns in elasmobranch fish. Microsc Res Tech 2002;59:396-407.
58. Takeyama K, Chatani M, Inohaya K, Kudo A. TGF-β2 signalling is essential for osteoblast migration and differentiation during fracture healing in medaka fish. Bone 2016;86:68-78.
59. Rash LJ, Martin KJ, Cooper RL, Metscher BD, Underwood CJ, Fraser GJ. An ancient dental gene-set governs development and continuous regeneration of teeth in sharks. Dev Biol 2016; 415:347-370.

new
STRONGER REPAIR

gsk

REPAIR & PROTECT

POWERED BY NOVAMIN

Nº1 DENTIST RECOMMENDED BRAND FOR SENSITIVE TEETH*

*Project Touchstone December 2016. For any product safety issues, contact GSK on +27 11 745 6001 or 0800 118 274